Optica Applicata, Vol. XXXVIII, No. 3, 2008

Characteristic analysis on an interleaver with a fiber loop resonator by using a signal flow graph method

WEIBIN LI[1, 2] , JUNQIANG SUN[1]

[1]Wuhan National Laboratory for Optoelectronics, School of Optoelectronic Science and Engineering, Huazhong University of Science and Technology, Wuhan 430074, Hubei, P.R. China

[2]Department of Physics and Chemistry, Henan Polytechnic University, Jiaozuo 454000, Henan, P.R. China

We propose an interleaver based on the Mach–Zehnder interferometer with a resonator incorporated in one arm. By using the method of signal flow graph, we get the simple closed-form expressions for transmission of this interleaver. The result indicates that the widths of 0.5 dB passband and 25 dB stopband of the interleaver are improved remarkably, which are much wider than that of the conventional Mach–Zehnder interferometer. The interleaver proposed has an ideal rectangular spectral response. Finally, we have analyzed the influence exerted by the parameters on its transimission characteristics and found that the transmission spectrum of this device depends highly on the intensity coupling coefficient of the coupler and fiber loop length.

Keywords: interleaver, resonator, signal flow graph, transmission.

1. Introduction

The dense wavelength division multiplexing (DWDM) is an effective method to increase the transmission capacity for optical communications. If one wishes to decrease the channel spacing in order to enlarge the transmission capacity, a so-called interleaver can be used to separate the input DWDM wavelengths into two interleaved sequences, and consequently, the channel spacing for each sequence is doubled as compared to the original DWDM channel spacing. This is a more cost-effective way to realize the DWDM technology with a narrow channel spacing [1, 2]. Because of this, it receives much attention in optical communication community. As regard the interleavers developed so far, most designs focus on Gires–Tournois based (GT-based) Michelson interferometer [1, 3], arrayed-waveguide router (AWG) [4, 5], ring resonator type filters [6], Mach–Zehnder interferometer (MZI) filters made with planar waveguides or fused fiber [7–9], and lattice filter employing birefringent

crystals [10], *etc*. Among those filters, the MZI filters are potential candidates, since they are inherently low loss, spectrally extremely selective, and potentially low cost. Furthermore, the MZIs have other important applications in optical nonlinearity measurement [11] and optical fiber sensing field [12]. So, the MZIs have attracted considerable interest.

In applications, the filters should have an ideal rectangular spectral response, *i.e*., large passband width with a flat top spectrum, and steep slope to achieve high isolation between adjacent channels over a large stopband region, which can relax the requirements on wavelength control for lasers. However, the spectral response of a conventional MZI is sinusoid, due to which the interleaver is limited in the bandwidth of passband/stopband. So, the conventional MZI is not appropriate for use. In order to obtain a flat-top passband, an interleaver based on cascaded MZIs is used [13]. A similar flat passband filter with 2×2 and 3×3 couplers has also been reported [14]. In this paper, we design a new modified project. An interleaver based on MZI with a fiber loop resonator in one arm is presented. The result indicates that the interleaver in this paper can simultaneously improve the widths of 0.5 dB passband and 25 dB stopband, which are much wider than those of the conventional Mach–Zehnder interferometer. The filtering performance of this novel interleaver, which achieves a nearly square spectrum response, is much better than that of the conventional MZI.

2. Theory and simulation analysis

Figure 1 shows a configuration of the interleaver proposed. It consists of an MZI with a ring resonator in one arm. The difference between this device and conventional MZI lies in a ring resonator used in one of the MZI arms. This can cause a multi-light beam interference effect, which results in the new change of phase between the two arms of MZI.

Various techniques have been used for the analysis of fiber optic and filter [15]. There are two main classes of such techniques. The first class comprises a set of analytical methods including the scattering matrix method, the transfer matrix/chain matrix algebraic method, and the method of solving the field equations. In the second class, use is made of a graphical approach; it is called the signal flow graph (SFG) method as proposed by MASON [16]. This method has originally been used in the electrical circuits, which is not a common practice in the analysis of optical circuits. The advantage of this method is that relations between unknown variables could be displayed explicitly and it provides better insight into the interaction of the system components. In addition, a set of equations corresponding to the graph can be easily derived by the association rule. This paper thus aims to employ this approach in the analytical derivation for the optical transfer functions of the structure proposed.

The SFG of the device is shown in Fig. 2. To determine the transmittance from node 1 to node 10, we examined all the paths going from node 1 to node 10 in the SFG.

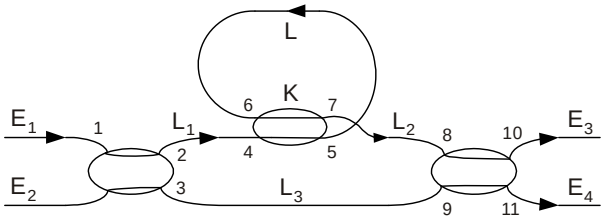

Fig. 1. Configuration of the MZI with a fiber loop resonator.

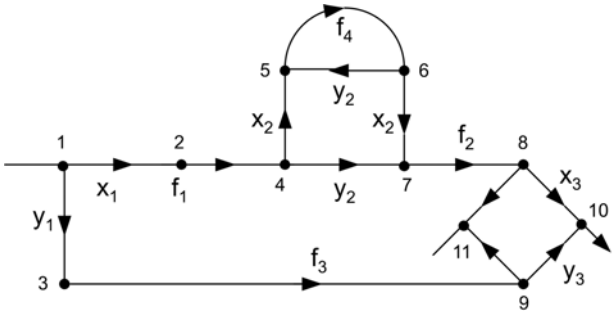

Fig. 2. SFG of the MZI with a ring resonator.

By inspection, there are three forward paths: P_1, 1 2 4 7 8 10; P_2, 1 2 4 5 f_4 6 7 8 10; P_3, 1 3 9 10. Because these paths are the product of their directed branches, respectively, P_1, P_2 and P_3 can be written as:

$$\begin{cases} P_1 = f_1 f_2 x_1 x_3 y_2 \\ P_2 = f_1 f_2 f_4 x_1 x_2^2 x_3 \\ P_3 = f_3 y_1 y_3 \end{cases} \tag{1}$$

where $x_i = (1 - k_i)^{1/2}$, $y_i = j(k_i)^{1/2}$ (i = 1, 2, 3), k_i is the intensity coupling coefficient of the corresponding coupler; and $f_i = \exp(i\beta L_i)$, L_i is the length of the fiber shown in Fig. 1, $f_4 = \exp(i\beta L)$, L is the fiber length of the fiber loop. In addition, we examined the SFG, with only one feedback loop, which is presented by nodes: 5 f_4 6 5. Its value is $y_2 f_4$. Also, we can see that only P_2 touches this feedback loop from the SFG. So, the Δ_i can be separately written as:

$$\begin{cases} \Delta_1 = 1 - y_2 f_4 \\ \Delta_2 = 1 \\ \Delta_3 = 1 - y_2 f_4 \end{cases} \tag{2}$$

Using the Mason rule, the transmission of the node 1 to 10 can be written as:

$$t = \frac{E_3}{E_1} = \frac{P_1\Delta_1 + P_2\Delta_2 + P_3\Delta_3}{\Delta} \tag{3}$$

with $\Delta = \Delta_1$. Using the above formulas, we obtain

$$T = \left|\frac{E_3}{E_1}\right|^3 = \frac{\frac{1}{2}(1+k) - \sqrt{k}\sin(\beta\Delta L) + \sqrt{k}\sin(\beta L) - \frac{1}{2}\cos\left[\beta(\Delta L - L)\right] + \frac{k}{2}\cos\left[\beta(\Delta L + L)\right]}{1 + k + 2\sqrt{k}\sin(\beta L)} \tag{4}$$

We assume 3 dB couplers are used in MZI. The optical fiber and coupler losses are neglected. The coefficient k is the intensity coupling coefficient of the coupler in the fiber loop resonator. $\Delta L = L_3 - L_1 - L_2$ is the pathlength difference of the two arms of MZI. Having satisfied the resonating condition, ΔL, $\Delta\lambda$ and L should satisfy the following relationships [8]:

$$\begin{cases} L = 2\Delta L - \dfrac{\lambda_0}{4n_{\text{eff}}} \\ \Delta L = \dfrac{\lambda_0^2}{n_{\text{eff}}\,\Delta\lambda} \end{cases} \tag{5}$$

with λ_0, n_{eff} and $\Delta\lambda$ standing for the center wavelength, the fiber effective index and the channel spacing, respectively.

Figure 3 shows the transmission spectra of MZI with a ring resonator as a function of frequency, where ΔL is set so as to obtain channel spacing of approximately 0.8 nm at center frequency $f_0 \approx 193.4$ THz (corresponding center wavelength $\lambda_0 = 1550$ nm). The intensity coupling coefficient k is 0.25 and n_{eff} is 1.47. It can be seen from Fig. 3 that the transmission spectrum of T is characterized by a series of equally spaced transmission peaks in the frequency domain, and the transfer function of rectangular--shaped frequency is accomplished.

For better understanding the filter characteristics of this device, the simulation results of a 25 dB stopband in 50 GHz channel spacing application are shown in Fig. 4. To have a closer look at the top portion of the spectra, Fig. 4**a** is enlarged and its top portion is shown in Fig. 4**b**. In these figures, the spectral response of the interleaver proposed is marked with solid line, and the dashed line represents a conventional MZI. It is clear that the flat-top ripple is less than 1.3×10^{-2} dB and the 0.5 dB passband width is about 42 GHz, which is near 84% of 50 GHz channel spacing. The 25 dB stopband width is found to be about 34 GHz (being nearly 68% of 50 GHz channel spacing).

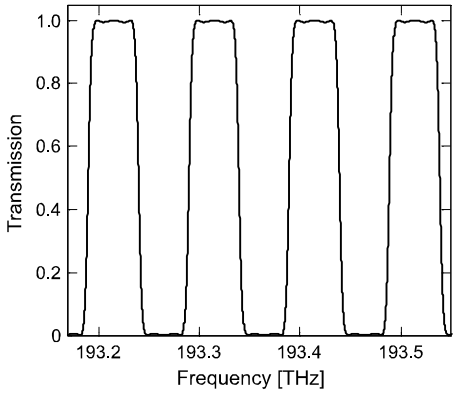

Fig. 3. Plot of transmission T versus frequency.

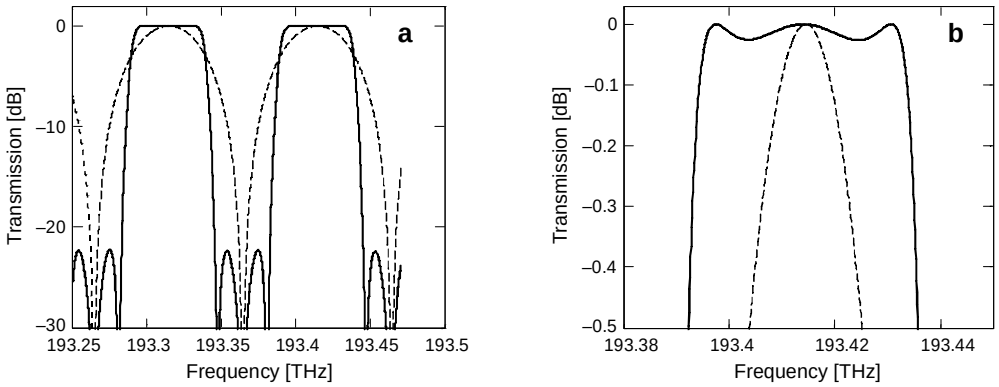

Fig. 4. Simulantion results of a 25 dB stopband (**a**) and a 0.5 dB passband (**b**) of the interleaver in 50 GHz channel spacing. Solid line: the interleaver proposed; dashed line: conventional MZI interleaver.

The channel isolation is, at least, to be better than 25 dB between the adjacent channels. The conventional MZI's 0.5 dB passband and 25 dB stopband widths are 21.4 GHz, 3.6 GHz, respectively. They correspondingly account for the 50 GHz channel spacing 42.8% and 7.2%. From Fig. 4, one can see that the interleaver proposed provides the 25 dB stopband and 0.5 dB passband widths, which are larger than those of conventional MZI. It is clear from the figures that the proposed interleaver is attractive in flat passbands. In addition, the 0.5 dB passband widths of the interleaver reported in [13, 14] are about 26 GHz and 33 GHz, and the 25 dB stopband widths are 24 GHz, 31 GHz, respectively. From this comparison, we can see that the interleaver proposed in this paper offers better filter effect.

From Eq. (4), we can see two new parameters, k and L, introduced in the device proposed. It is necessary to study the influence of these parameters on transimission characteristics of the interleaver proposed.

In Figure 5, transmission spectra of T versus frequency, with different k, are presented. The B, C, D, E, F correspond to the values of intensity coupling coefficient k for 1/4, 1/2, 3/4, 7/8 and 1. It is clear from the figure that all the curves intersect at

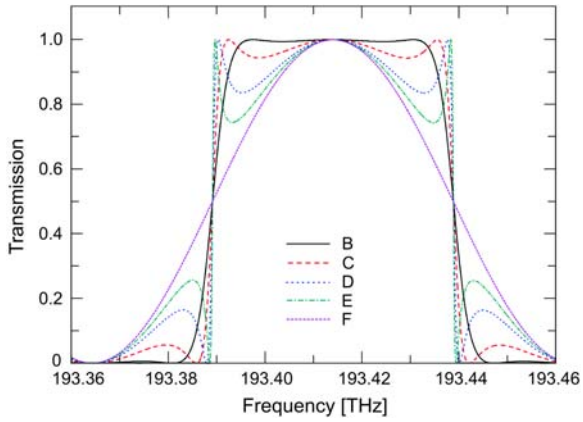

Fig. 5. Transmission spectrum T versus frequency with different k; B, C, D, E, F correspond to the values of k for 1/4, 1/2, 3/4, 7/8 and 1.

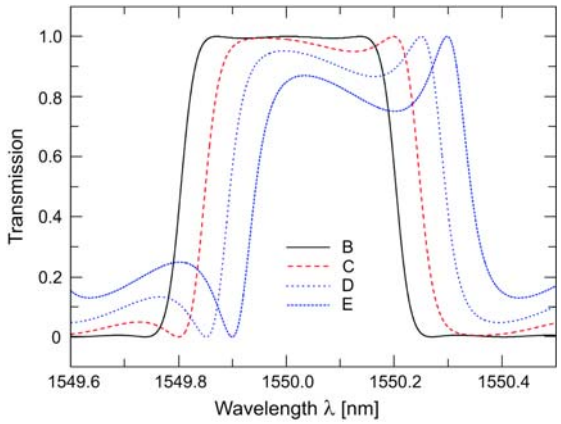

Fig. 6. The transmission spectra of interleaver with different L; B, C, D, E correspond to the change of L, which are 0, 100, 200, 300 nm, respectively.

half maximum intensity 1/2, and the intensity in the passband and that in the stopband of the interleaver are complementary. Note that the curve with $k = 1$ restores to that of conventional MZI. In addition to this, when $k = 0$, the transmission spectra are also those of the conventional MZI. This is because the multilight beam interference has not been produced in the fiber loop resonator, and thus the proposed interleaver is equivalent to the conventional MZI. From the figure, it can also be seen that as the value of k increases, one peak and one trough symmetrically appear on either side of the center frequency; these extreme points move outwards and the trough gets deeper, resulting in a wider bandwidth but with a large ripple. Besides, with an increase of k, the side lobe is enhanced, which results in the channel isolation reduction. So, in the real-world application, k should take a small value to satisfy a given isolation requirement.

Because the transmission spectrum of interleaver is sensitive to the length of fiber loop, the system has strict request for the optical fiber loop length. In order to show how big this kind of influence is, we have drawn transmission spectra of the interleaver proposed with different L in Fig. 6. The parameters in the figure are: $\Delta L \approx 2.05$ mm, $L \approx 4.1$ mm, $\lambda_0 = 1550$ nm, $k = 0.25$ and $\Delta\lambda = 0.8$ nm; *B* denotes the curve when L is 4.1 mm; *C*, *D*, *E* are the curves when the length changes are 100 nm, 200 nm and 300 nm, respectively. One can see in the figure one trough appearing on the right-hand side of the center wavelength with L increasing. This causes the ripple to increase. It can also be seen that as the value of L increases, the side lobe is enhanced, which results in the channel isolation reduction. Furthermore, the center wavelength shows the drifting along the long wave direction. The cause of these phenomena is that matching condition, $L = 2\Delta L - \lambda_0/(4n_{\text{eff}})$, has been destroyed with the change of L. In brief, when L changes, the shape of the curve is distorted. In order to achieve the best system performance, the L drifting should be smaller than 100 nm by our calculation.

3. Conclusions

In this paper, we have proposed a novel interleaver based on MZI with a fiber loop resonator in one arm. The interleaver can have the widths of 0.5 dB passband and 25 dB stopband simultaneously improved, which are much wider than those of conventional Mach–Zehnder interferometer. The interleaver proposed has an ideal rectangular spectral response, *i.e.*, large passband bandwidth with a flat top spectrum, steep slope and high isolation. This performance can relax the requirements on wavelength control for lasers in a DWDM system. Finally, we have analyzed the influence exerted by the parameters on its transimission characteristics and found that the transmission spectrum of this device depends highly on the intensity coupling coefficient of the coupler and fiber loop length. The calculation and analysis in this paper aim at the optical fiber, and the interleaver may be realized by using the plane waveguide technology.

References

[1] HSIEH C.-H., WANG R., WEN Z.J., MCMICHAEL I., YEH P., LEE C.-W., CHENG W.-H., *Flat-top interleavers using two Gires–Tournois etalons as phase-dispersive mirrors in a Michelson interferometer*, IEEE Photonics Technology Letters **15**(2), 2003, pp. 242–44.

[2] MIZUNO T., KITOH I., SAIDA I., OGUMA M., SHIBATA T., HIBINO Y., *Dispersionless interleave filter based on transversal form optical filter*, Electronics Letters **38**(19), 2002, pp. 1121–22.

[3] DINGEL B.B., IZUTSU M., *Multifunction optical filter with a Michelson–Gires–Tournois interferometer for wavelength-division-multiplexed network system applications*, Optics Letters **23**(14), 1998, pp. 1099–101.

[4] OKAMOTO K., SUGITA A., *Flat spectral response arrayed-waveguide grating multiplexer with parabolic waveguide horns*, Electronics Letters **32**(18), 1996, pp. 1661–2.

[5] AMERSFOORT M.R., SOOLE J.B.D., LEBLANC H.P., ANDREADAKIS N.C., RAJHEL A. CANEAU C., *Passband broadening of integrated arrayed waveguide filters using multimode interference couplers*, Electronics Letters **32**(5), 1996, pp. 449–51.

[6] KOHTOKU M., OKU S., KADOTA Y., SHIBATA Y., YOSHIKUNI Y., *200-GHz FSR periodic multi/demultiplexer with flattened transmission and rejection band by using a Mach–Zehnder interferometer with a ring resonator*, IEEE Photonics Technology Letters **12**(9), 2000, pp. 1174–6.
[7] OGUMA M., JINGUJI K., KITOH T., SHIBATA T., HIMENO A., *Flat-passband interleave filter with 200 GHz channel spacing based on planar lightwave circuit-type lattice structure*, Electronics Letters **36**(15), 2000, pp. 1299–300.
[8] JINGUJI K., OGUMA M., *Optical half-band filters*, Journal of Lightwave Technology **18**(2), 2000, pp. 252–9.
[9] WANG Q.J., ZHANG Y., SOH Y.C., *All-fiber 3×3 interleaver design with flat-top passband*, IEEE Photonics Technology Letters **16**(1), 2004, pp. 168–70.
[10] DAMASK J.N., DOERR C.R., *Polarization diversity for birefringent filters*, US Patent 6252711, B1. 2001.
[11] VINEGONI C., WEGMULLER M., GISIN N., *Measurements of the nonlinear coefficient of standard, SMF, DSF, and DCF fibers using a self-aligned interferometer and a Faraday mirror*, IEEE Photonics Technology Letters **13**(12), 2001, pp. 1337–9.
[12] SONG M., YIN S., RUFFIN P.B., *Fiber Bragg grating strain sensor demodulation with quadrature sampling of a Mach–Zehnder interferometer*, Applied Optics **39**(7), 2000, pp. 1106–11.
[13] HUAI-WEI LU, YU-E ZHANG, GUAN-WEI LUO, *Study of all-fiber flat-top passband interleaver based on 2×2 and 3×3 fiber couplers*, Optics Communications **276**(1), 2007, pp. 116–21.
[14] HUAI-WEI LU, BAO-GE ZHANG, MIN-ZHI LI, GUAN-WEI LUO, *A novel all-fiber optical interleaver with flat-top passband*, IEEE Photonics Technology Letters **18**(13), 2006, pp. 1469–71.
[15] YUPAPIN P.P., SAEUNG P., LI C., *Characteristics of complementary ring-resonator add/drop filters modeling by using graphical approach*, Optics Communications **272**(1), 2007, pp. 81–6.
[16] MASON S.J., *Feedback theory – further properties of signal flow graphs*, Proceedings of the IRE **44**(7), 1956, pp. 920–6.

Received February 26, 2008